SUPPORTING INFORMATION

Assembly-mediated Interplay of Dipolar Interactions and Surface Spin Disorder in Colloidal Maghemite Nanoclusters

A. Kostopoulou,[a] K. Brintakis,[a,b] M. Vasilakaki,[c] K.N. Trohidou,[c] A.P. Douvalis,[d] A. Lascialfari,[e] L. Manna [f] and A. Lappas *[a]

[a] Institute of Electronic Structure and Laser, Foundation for Research and Technology-Hellas, Vassilika Vouton, Heraklion 71110, Greece.
Fax: +30 2810 301305; Tel: +30 2810 391344; E-mail: lappas@iesl.forth.gr

[b] Department of Physics, Aristotle University of Thessaloniki, 54124 Thessaloniki, Greece.

[c] IAMPPNM, Department of Materials Science, NCSR "Demokritos", Aghia Paraskevi, 15310, Athens, Greece.

[d] Department of Physics, University of Ioannina, Ioannina 45110, Greece.

[e] Dipartimento di Fisica, Università degli studi di Milano and INSTM, Via Celoria 16, I-20133 Milano, Italy.
[f] Istituto Italiano di Tecnologia, Via Morego 30, 16163 Genova, Italy.

Corresponding Author
lappas@iesl.forth.gr

Colloidal Stability of the Nanoclusters (CNCs) through Dynamic Light Scattering (DLS) and z-potential measurements.

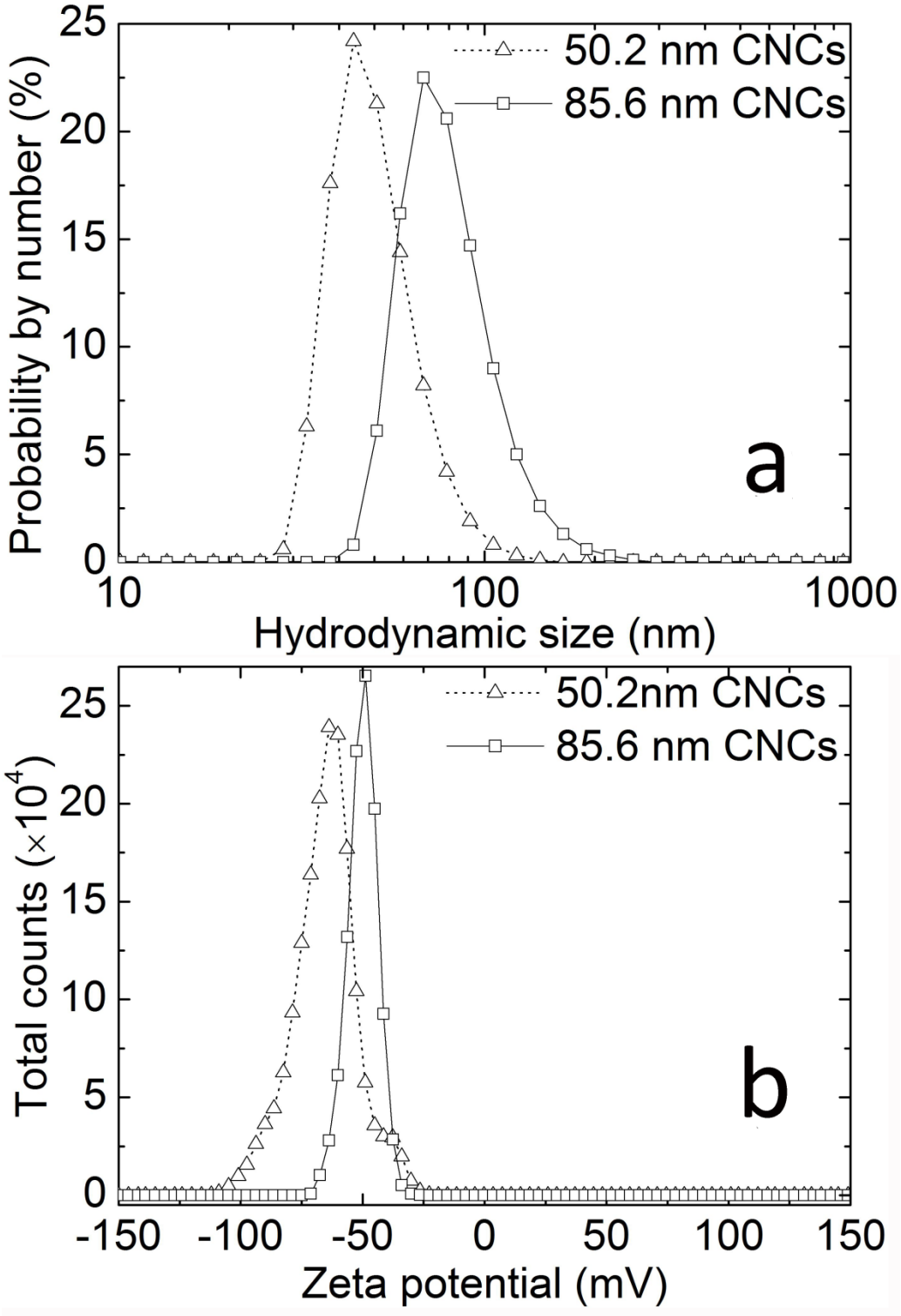

Fig. S1. Size distribution by DLS (a) and the z-potential (b) of CNCs with diameters 50.2 (triangles) and 85.6 nm (squares).

Table S1. Comparison of the average diameters (D) of the CNCs by TEM and DLS. The latter is given by number and by intensity and shows a narrow size distribution with low polydispersity (PdI index).

D_{TEM} (nm)	Standard deviation by TEM (nm)	$D_{DLS/number}$ (nm)	$D_{DLS/intensity}$ (nm)	PdI_{DLS}
50.2	5.4	51.0	78.6	0.1
85.6	13.3	81.8	121.8	0.2

Determination of the chemical nature of the CNCs by the Mössbauer technique.

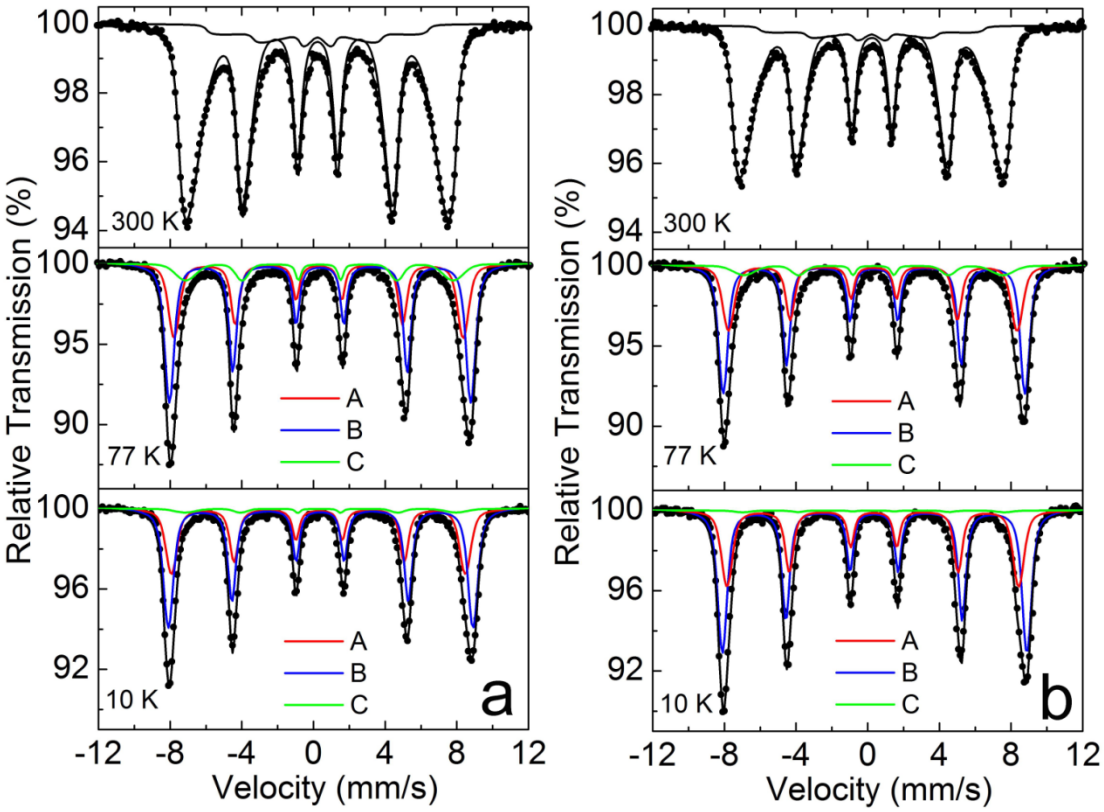

Fig. S2. ^{57}Fe Mössbauer spectra of the 50.2 (a) and 85.6 nm (b) CNCs recorded at different temperatures. Two components were employed in fitting the spectra at 300 K and three at 77 K and 10 K.

All the ^{57}Fe Mössbauer spectra (MS) were magnetically split, with increased line broadening at 300 K. In an effort to fit the room temperature MS a set of two magnetically split components, with asymmetric spreading of their hyperfine magnetic field (B_{hf}) values (Gaussian-type, ΔB_{hf}) was employed. Nonetheless, the component with the minority absorption area was showing collapsing B_{hf} characteristics in both samples. As the temperature was decreased the spectral lines became more symmetric and the two main sextets A and B, with raised B_{hf} and diminished ΔB_{hf} values (Table S2), respectively, dominated the spectra. Importantly, we found that the isomer shift (IS) values for all components (Table S2) are typical of Fe^{3+} ions in oxygen coordinated environment.[1] The two distinguished main components (A and B) at the 10 and 77 K MS can be attributed to the characteristic tetrahedral (A) and octahedral (B) Fe^{3+} ion crystal sites and further indicate a relative narrow dispersion of primary nanocrystal sizes.[1, 2] The C component corresponds either to the smaller NPs incorporated in the CNCs, whose reduced size restrict them from developing the A- and B- site characteristics of the larger NPs, or to not fully ferrimagnetically aligned (frustrated) surface spins of the NPs . At room temperature, the faster superparamagnetic relaxation due to increased thermal agitation, gives rise to Mössbauer spectral lines that are too broad to clearly distinguish the Fe^{3+} A- and B- sites of the spinel structure. [3, 4]

Table S2. ^{57}Fe Mössbauer parameters as resulted from the best fit of the corresponding spectra. T, IS, Γ/2, QS-2ε, B_{hf}, ΔB_{hf}, Area and Comp., correspond to temperature, isomer shift, half line-width, quadrupole splitting-shift, hyperfine magnetic field, spread of the hyperfine magnetic field, relative absorption area and component assignment, respectively. At 300 K the asymmetric spreading around the central B_{hf} value is given by two ΔB_{hf} values, ΔB_{hf}-lower/ΔB_{hf}-higher than B_{hf}, and once the ΔB_{hf}-higher value is resulting to 0, the spreading is essentially confined in values lower than B_{hf}.

NPs or CNCs size, D (nm)	T (K)	IS (mm/s)	Γ/2 (mm/s)	QS or 2ε (mm/s)	B_{hf} (T)	ΔB_{hf} (T)	Area (%)	Comp.
12.7	300	0.38	0.46	-0.01	48.2	5.5/0.0	73	
		0.38	0.25	-0.01	16.3	10.3	24	
		0.38	0.35	0.70	0.0	0.0	3	
50.2	300	0.33	0.25	0.00	47.8	2.7/0.0	88	
		0.33	0.19	0.00	38.0	10.0/0.0	12	
	77	0.40	0.21	-0.02	50.1	1.3	33	A
		0.47	0.21	0.00	52.2	1.0	55	B
		0.45	0.13	0.00	46.4	3.2	12	C
	10	0.40	0.22	-0.04	51.0	1.3	36	A
		0.49	0.22	0.03	52.8	1.0	61	B
		0.47	0.12	0.08	47.0	3.4	3	C
85.6	300	0.33	0.23	-0.01	47.9	2.7/0.0	89	
		0.33	0.19	0.00	38.4	10.1/0.0	11	
	77	0.42	0.21	-0.06	50.0	1.4	35	A
		0.46	0.21	0.01	52.3	0.9	57	B
		0.43	0.14	0.00	44.9	3.4	8	C
	10	0.42	0.22	-0.05	50.6	1.2	37	A
		0.48	0.22	0.03	52.8	0.9	62	B
		0.44	0.26	0.00	45.5	2.0	1	C

Frequency dependent real part of the ac susceptibility, χ'(T).

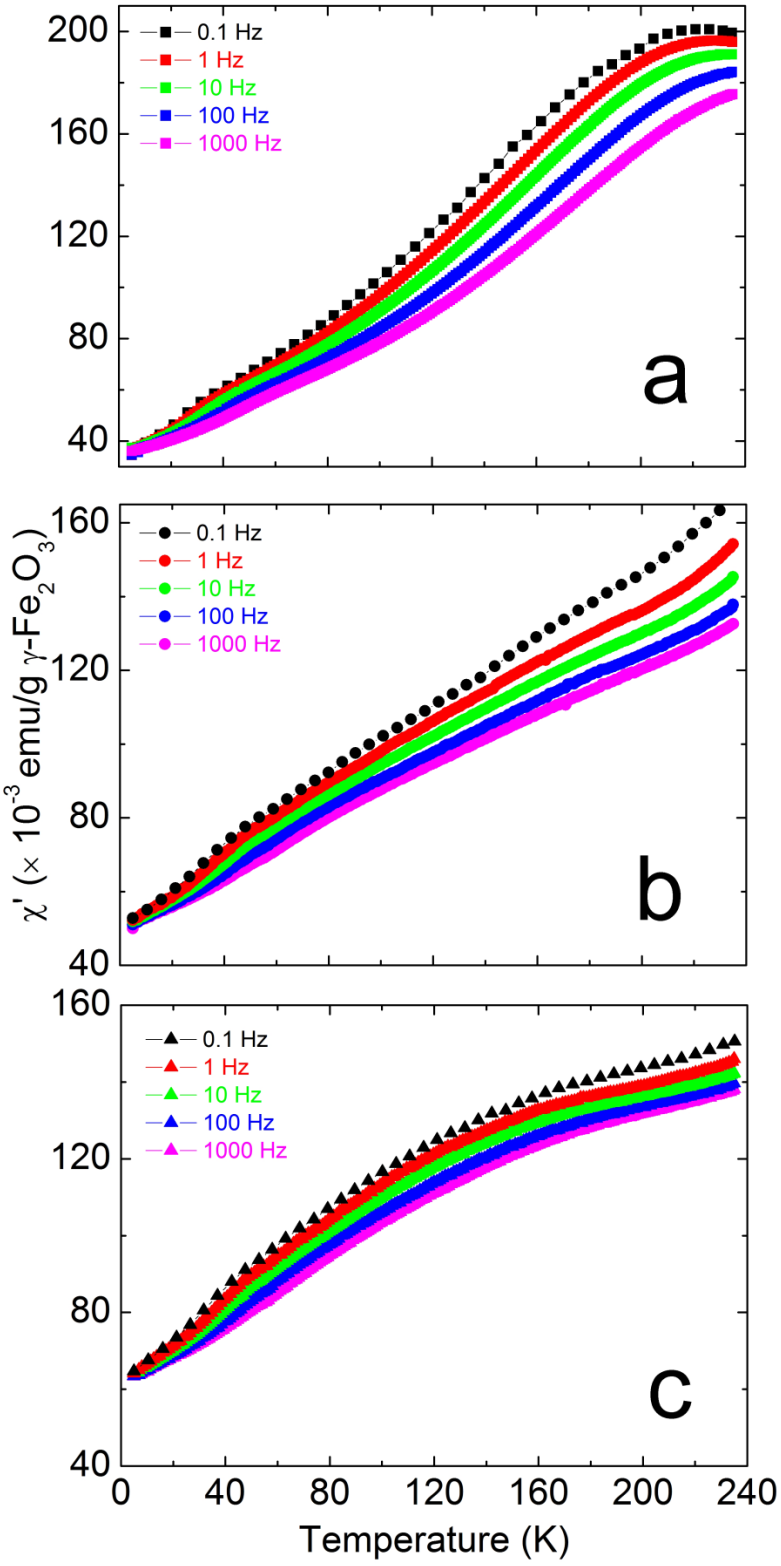

Fig. S3 Frequency dependent real, χ'(T), part of the ac susceptibility, for the 12.7 nm individual NPs (a), the 50.2 nm (b) and 85.6 nm (c) CNCs samples in solution form.

Phenomenological-law analysis of the frequency dispersion of the high and low temperature χ''(T) maxima.

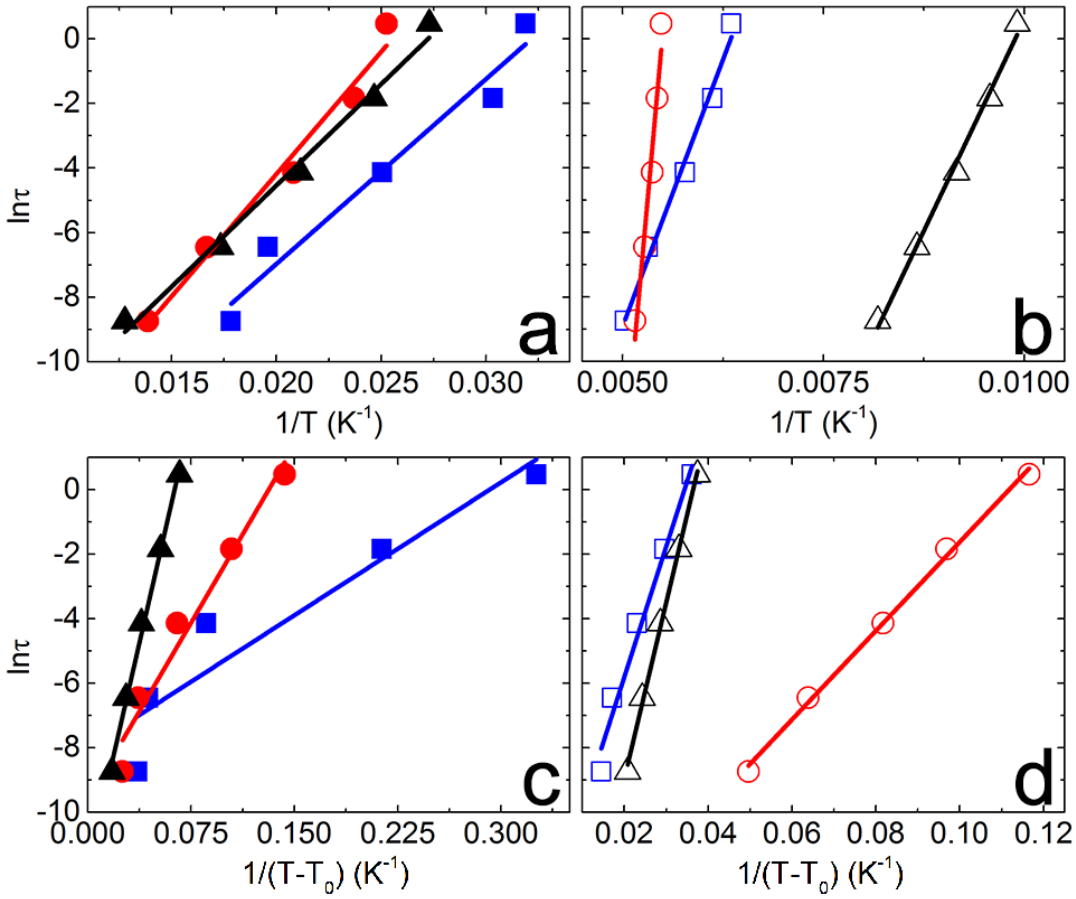

Fig. S4 Arrhenius and Vogel-Fulcher law description of the frequency dispersion of the low (a, c) and high (b, d) temperature χ''(T) maxima in the 12.7 nm individual NPs (squares), the 50.2 nm CNCs (circles), 85.6 nm (triangles) CNCs samples.

Determination of the freezing point of the CNCs.

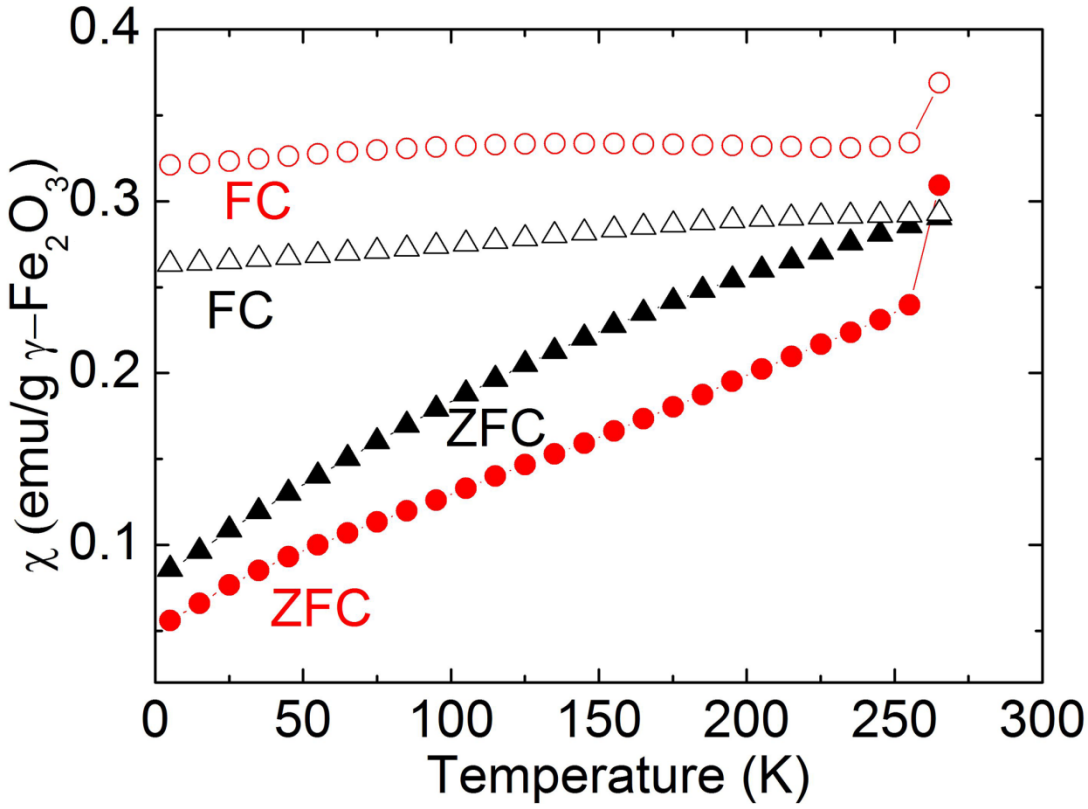

Fig. S5. ZFC (filled points) and FC (open points) susceptibility, χ, as function of temperature for the 50.2 (circles) and 85.6 nm (triangles) CNCs frozen aqueous solution under a magnetic field of 50 Oe.

The jump in the ZFC susceptibility curve at 255 K for the small CNCs is due to the transformation (melting) of the frozen solution to liquid, suggesting that the nanoclusters become free to align along the field.[5] The freezing points of the CNCs aqueous solutions are below that of the water due the existence of minute amount of PAA left over, which varies between the two dispersions. It is worth noting that the average mass contribution of the polyacrylate surfactant layer of the CNCs has been estimated to be 7.9 % for the large CNCs and 13.2 % for the small CNCs through thermogravimetric measurements. Our estimate of the freezing point of the solution for the small and the large CNCs is 255 K and greater than 265 K, respectively.

Determination of the inter-cluster interaction strength with Mössbauer spectroscopy.

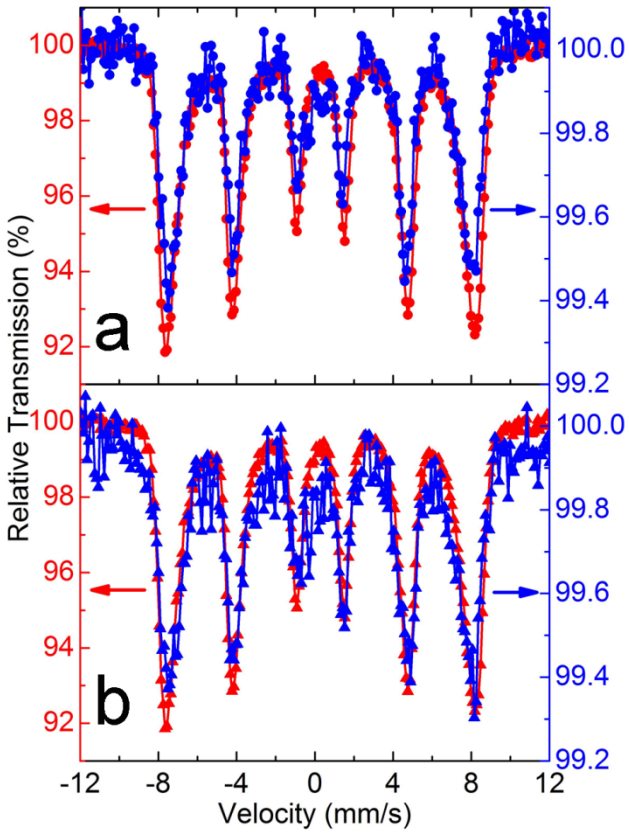

Fig. S6. Comparison of the ^{57}Fe Mössbauer raw spectra for the dried powder (red lines) and the corresponding frozen solution (blue lines) for the 50.2 (a) and 85.6 nm (b) CNCs samples at 200 K.

Monte Carlo simulations of individual NPs with only one spin and with 3 spins and surface spin disorder.

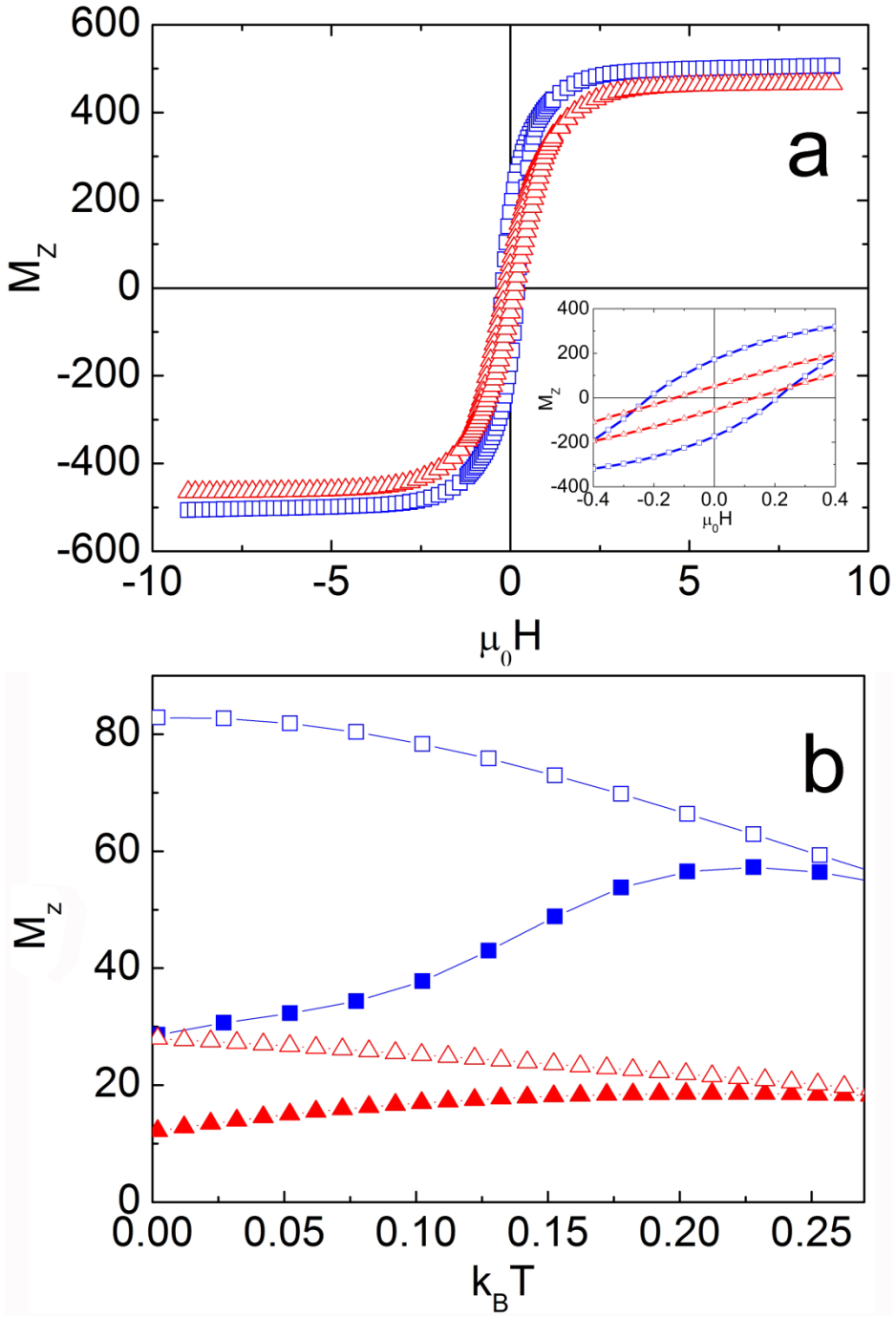

Fig. S7: Monte Carlo simulated isothermal magnetization curves (a) at T= 0.05, zero-field (ZFC) and field-cooled (FC) magnetization curves (b) for the 12.7 nm individual NPs (p= 0.47) with core/surface morphology (squares) and with only one spin with random anisotropy (Stoner Wohlfarth model) (triangles).

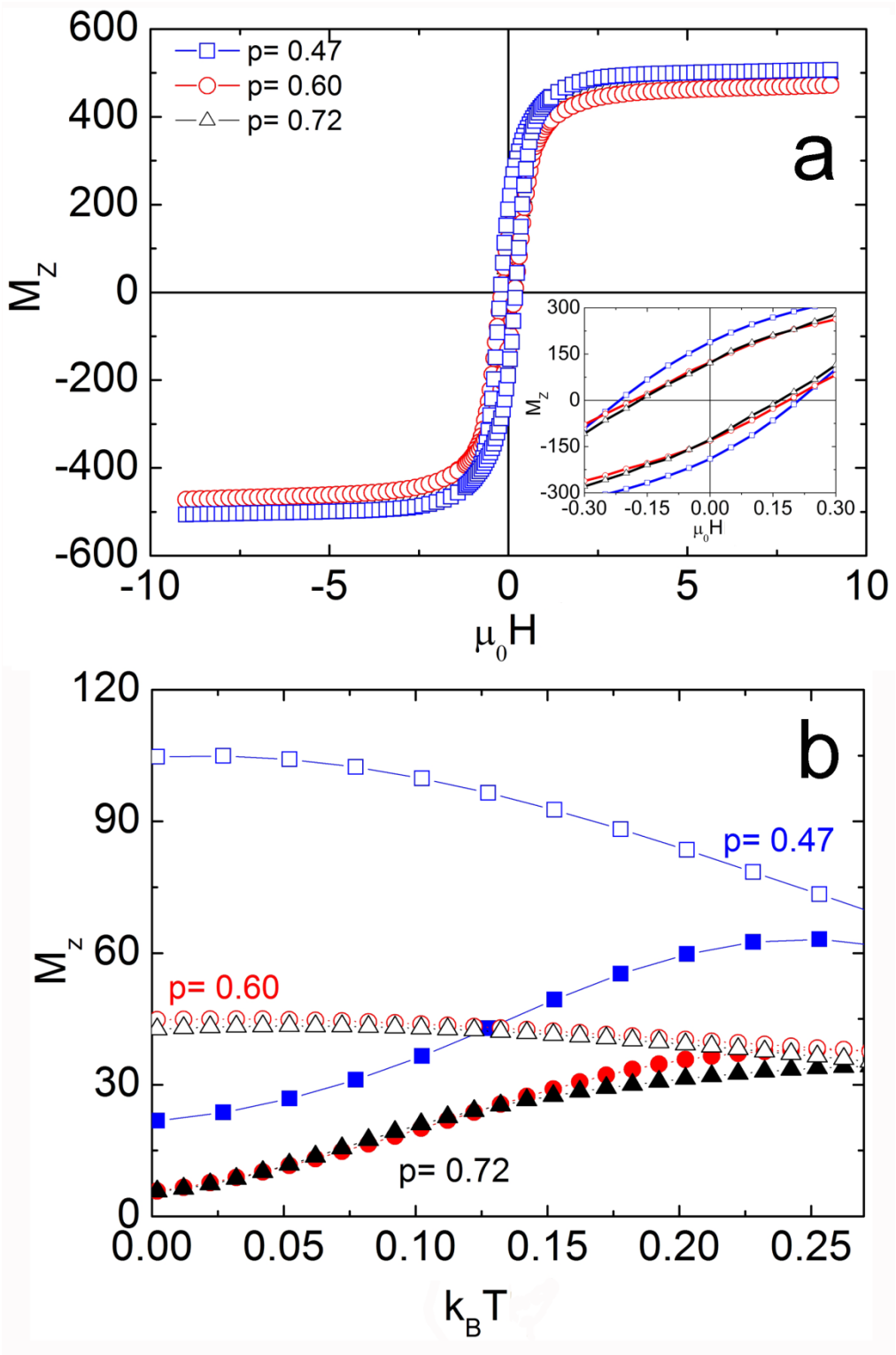

Fig. S8: Monte Carlo simulated isothermal magnetization curves (a) at T= 0.05 (a), zero-field (ZFC) and field-cooled (FC) magnetization curves (b) for the 12.7 nm individual NPs (p= 0.47) with core/surface morphology with a disordered spin arrangement (case analogous to the CNCs).

Monte Carlo simulations with dipolar interactions (g) or the intra-particle spin-exchange interactions (J_{13}, J_{12}, J_{23}) "switched off".

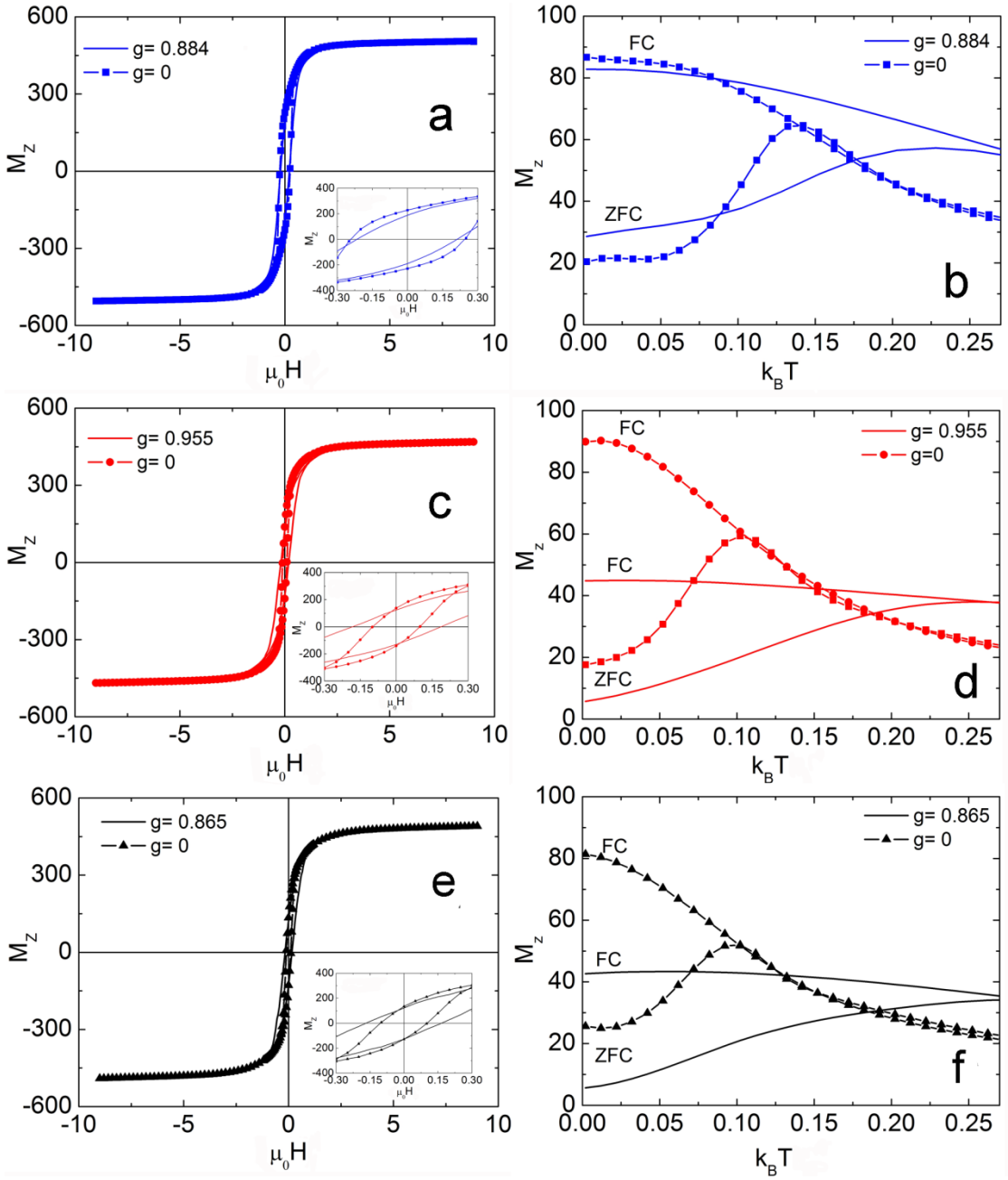

Fig. S9: Monte Carlo simulated isothermal magnetization curves at T= 0.05, zero-field (ZFC) and field-cooled (FC) magnetization curves for individual nanoparticles (p= 0.47) (a, b), and cluster type systems with p= 0.60 (c, d) and p= 0.72 (e, f), for the original model (g≠ 0; lines) and when the dipolar interactions are switched off (g= 0; lines with symbols).

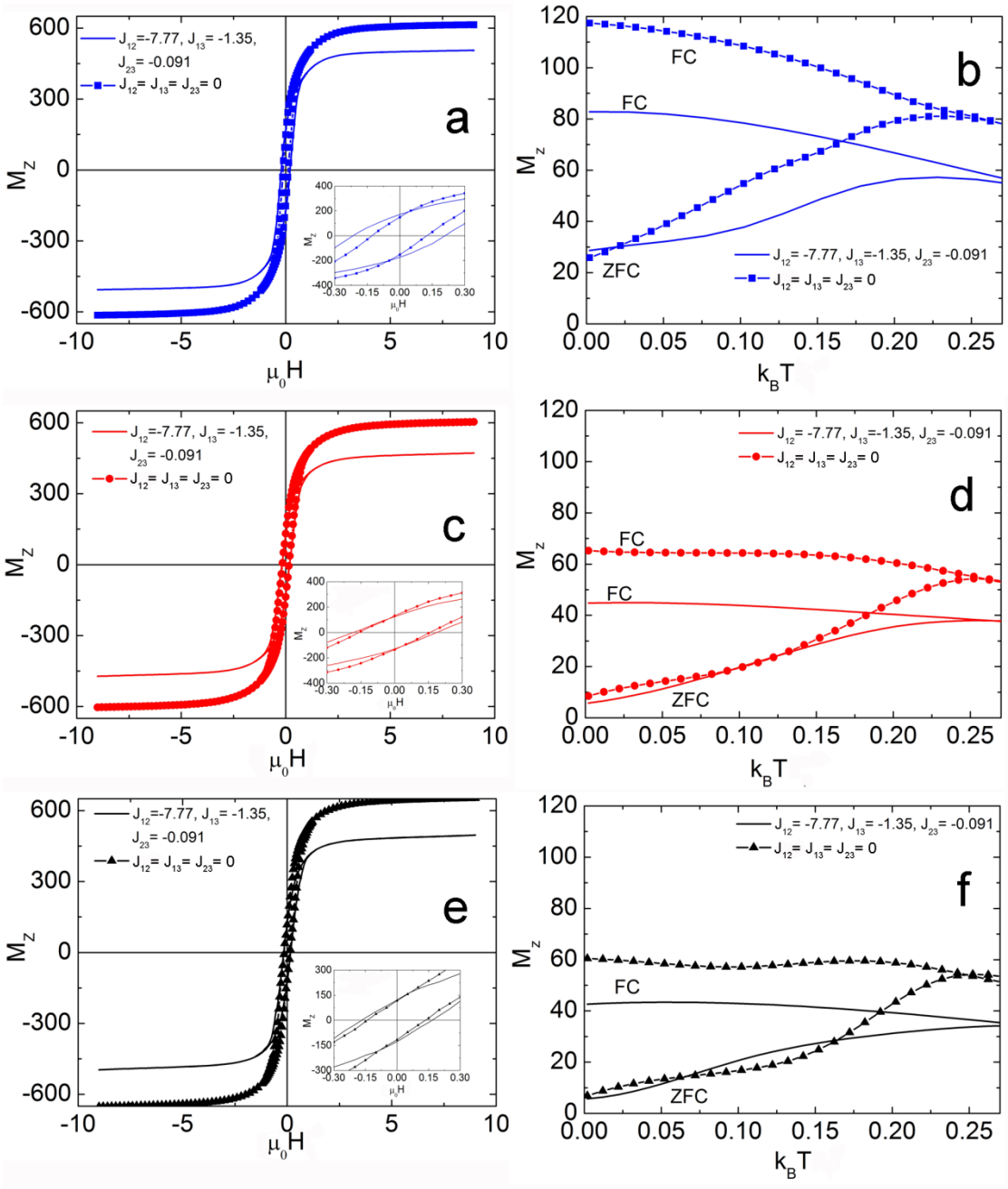

Fig. S10: Monte Carlo simulated isothermal magnetization curves at T= 0.05, zero-field (ZFC) and field-cooled (FC) magnetization curves for individual nanoparticles (p= 0.47) (a, b), and cluster type systems with p= 0.60 (c, d) and p= 0.72 (e, f), for the original model (J_{12}, J_{13}, J_{23} non-zero; lines) and when the intra-particle interactions are switched off (, J_{12}=J_{13}=J_{23}= 0; lines with symbols).

References

1. N. N. Greenwood and T. C. Gibb, *Mössbauer Spectroscopy*, Chapman and Hall: London, 1971.
2. R. M. Cornell, Schwertmann, U., *The Iron Oxides: Structure, Properties, Reactions, Occurancies and Uses*, Wiley VCH Verlag: Weiheim, 2003.
3. S. Mørup, *Hyperfine Interact*, 1990, **60**, 959.
4. S. A. Corr, Y. K. Gun'ko, A. P. Douvalis, M. Venkatesan, R. D. Gunning and P. D. Nellist, *J Phys Chem C*, 2008, **112**, 1008.
5. J. Tejada, R. F. Ziolo and X. X. Zhang, *Chem Mater*, 1996, **8**, 1784.